Check for updates

RESEARCH ARTICLE

Ca^{2+}–Calmodulin–Calcineurin Signaling Modulates α-Synuclein Transmission

Jun Ueda, MD, PhD, Norihito Uemura, MD, PhD,* Tomoyuki Ishimoto, MD, Tomoyuki Taguchi, MD, PhD, Masanori Sawamura, MD, PhD, Etsuro Nakanishi, MD, PhD, Masashi Ikuno, MD, PhD, Shuichi Matsuzawa, PhD, Hodaka Yamakado, MD, PhD, and Ryosuke Takahashi, MD, PhD*

Department of Neurology, Kyoto University Graduate School of Medicine, Kyoto, Japan

ABSTRACT: Background: The intercellular transmission of pathogenic proteins plays a crucial role in the progression of neurodegenerative diseases. Previous research has shown that the neuronal uptake of such proteins is activity-dependent; however, the detailed mechanisms underlying activity-dependent α-synuclein transmission in Parkinson's disease remain unclear.
Objective: To examine whether α-synuclein transmission is affected by Ca^{2+}–calmodulin–calcineurin signaling in cultured cells and mouse models of Parkinson's disease.
Methods: Mouse primary hippocampal neurons were used to examine the effects of the modulation of Ca^{2+}–calmodulin–calcineurin signaling on the neuronal uptake of α-synuclein preformed fibrils. The effects of modulating Ca^{2+}–calmodulin–calcineurin signaling on the development of α-synuclein pathology were examined using a mouse model injected with α-synuclein preformed fibrils.
Results: Modulation of Ca^{2+}–calmodulin–calcineurin signaling by inhibiting voltage-gated Ca^{2+} channels, calmodulin, and calcineurin blocked the neuronal uptake of α-synuclein preformed fibrils via macropinocytosis. Different subtypes of voltage-gated Ca^{2+} channel differentially contributed to the neuronal uptake of α-synuclein preformed fibrils. In wild-type mice inoculated with α-synuclein preformed fibrils, we found that inhibiting calcineurin ameliorated the development of α-synuclein pathology.
Conclusion: Our data suggest that Ca^{2+}–calmodulin–calcineurin signaling modulates α-synuclein transmission and has potential as a therapeutic target for Parkinson's disease. © 2023 The Authors. *Movement Disorders* published by Wiley Periodicals LLC on behalf of International Parkinson and Movement Disorder Society.

Key Words: Parkinson's disease; α-synuclein; propagation; micropinocytosis; Ca^{2+}–calmodulin–calcineurin signaling

Introduction

Parkinson's disease (PD) is one of the most common neurodegenerative diseases. The presence of Lewy bodies, composed of misfolded and fibrillized α-synuclein (α-syn), is a pathological feature of PD. There is growing evidence that the interneuronal propagation of misfolded α-syn underlies the progression of PD.[1-8] In this scenario, the misfolded α-syn works as a template to recruit normal endogenous α-syn to the misfolded α-syn aggregates in neurons. The misfolded α-syn is then released into the extracellular space and taken up by adjacent neurons, followed by further α-syn misfolding and aggregation in these neurons. Recently, we

This is an open access article under the terms of the Creative Commons Attribution-NonCommercial-NoDerivs License, which permits use and distribution in any medium, provided the original work is properly cited, the use is non-commercial and no modifications or adaptations are made.

*Correspondence to: Dr. Norihito Uemura and Ryosuke Takahashi, Department of Neurology, Kyoto University Graduate School of Medicine, 54 Shogoin, Kawaramachi, Sakyo-ku, Kyoto, 606-8507, Japan; E-mail: nuemura@kuhp.kyoto-u.ac.jp and ryosuket@kuhp.kyoto-u.ac.jp

Relevant conflicts of interest/financial disclosures: None.

Funding Agencies: This study was supported by a grant from the Ministry of Education, Culture, Sports, Science, and Technology (NJP22K20683 Grant-in-Aid for Research Activity Start-up; JP18H04041, Grant-in-Aid for Scientific Research on Innovative Areas), and the Integrated Neurotechnologies for Disease Studies (Brain/MINDS) from Japan Agency for Medical Research and Development AMED (RT, JP19dm0207070).

Received: 21 November 2022; **Revised:** 8 March 2023; **Accepted:** 20 March 2023

Published online 17 April 2023 in Wiley Online Library (wileyonlinelibrary.com). DOI: 10.1002/mds.29401

demonstrated that an α-amino-3-hydroxy-5-methyl-4-isoxazolepropionic acid (AMPA) receptor antagonist, perampanel (PER), inhibits the formation of phosphorylated α-syn (p-α-syn) aggregates by lowering the activity-dependent neuronal uptake of α-syn preformed fibrils (PFFs) via macropinocytosis.[9] Moreover, recent studies have also confirmed that activity-dependent mechanisms mediate the neuronal uptake of α-syn PFFs.[10,11] However, it remains unclear how neuronal activity affects neuronal α-syn PFFs uptake.

Voltage-gated Ca^{2+} channels (VGCCs), classified into L-, N-, P/Q-, R-, and T-type channels based on their electrophysiological and pharmacological properties, are regulated by neuronal activity. The influx of Ca^{2+} via VGCCs activates calmodulin (CaM) and calcineurin (CaN), which are strongly involved in endocytic processes.[12,13] However, the association between neuronal α-syn PFFs uptake and Ca^{2+}–CaM–CaN signaling warrants clarification. Therefore, in this study, we examined the contribution of Ca^{2+}–CaM–CaN signaling to α-syn PFFs uptake and the subsequent development of α-syn pathology in PD models.

Materials and Methods

Animals

Male C57BL/6J mice (n = 68; age, 2-3 months) were provided by Shimizu Laboratory Supplies or CLEA Japan. The Kyoto University Animal Care and Use Committee approved the breeding, housing, and experimental procedures, which were carried out as per the guidelines.

Preparation of Recombinant α-Syn Monomers and PFFs

Mouse α-syn PFFs were produced using previously described methods.[14] Before the administration of α-syn PFFs, we sonicated them with a Bioruptor bath sonicator for 10 minutes (30 seconds of sonication followed by an interval of 30 seconds).

Stereotaxic Injection

Previously described methods were used to perform stereotaxic injection.[15,16] Using a 33-gauge microsyringe, isoflurane-anesthetized mice were stereotaxically injected with 0.5 μL of α-syn PFFs (5 mg/mL) bilaterally into the olfactory bulb (OB) (coordinates: AP: +4.5 mm, L or R: −0.9 mm, DV: −1.5 mm relative to the bregma and skull surface).

CaN Activity Assay

CaN activity in mouse brain tissue was measured using a Calcineurin Cellular Assay Kit (Enzo Life Sciences, Inc., USA) according to the manufacturer's instructions. Brain tissues of mice treated with cyclosporin A (CyA) or vehicle (n = 9) were used. CaN activity was measured as the dephosphorylation rate of a synthetic phosphopeptide substrate.

Immunohistochemistry

Previously described immunohistochemistry procedures were used, with minor variations.[14,15] Briefly, mice were sacrificed 2 weeks after α-syn PFFs injection. After fixing with 4% paraformaldehyde (PFA), the brains were embedded in paraffin and cut into 8 μm-thick sections. Antibodies against p-α-syn (1:5000; ab51253, Abcam, UK), glial fibrillary acidic protein (GFAP) (1:1000; G3893, Sigma–Aldrich, USA), and ionized calcium-binding adaptor protein-1 (Iba-1) (1:1000; 019-19,741, Wako, Japan) were used as primary antibodies. The ImageJ software was used to quantify the p-α-syn-, GFAP-, and Iba-1-positive areas in the anterior olfactory nucleus (AON), and the total number of neuronal p-α-syn-positive aggregates was manually counted. Coronal sections at +3.08, +2.80, and +2.58 mm relative to the bregma were used to evaluate the AON pathology.

CyA Treatment

CyA powder was suspended in a 0.5% (w/v) methylcellulose solution (final concentration of CyA: 100 mg/mL; Wako, Japan). Mice were orally administered with 10 μL of CyA/g of body weight daily. The mice were administered with 100 mg/kg CyA (CyA, n = 7) or vehicle (control, n = 7) before the injection of α-syn PFFs. The dose of CyA was determined based on a previous report.[17] After α-syn PFFs injection, treatment with CyA or vehicle was continued for 2 weeks.

Sequential Extraction

The mouse brains were extracted sequentially, as described previously.[18] For biochemical analysis, we dissected the ventral half of the cerebral cortex containing the AON from phosphate-buffered saline (PBS)-perfused brains of mice treated with 100 mg/kg CyA or vehicle for 1 week without α-syn PFFs inoculation (n = 8, respectively) (Fig. 5C,D) and mice treated with 100 mg/kg CyA or vehicle for 2 weeks after α-syn PFFs injection into the OB (n = 5, respectively) (Fig. 5I).

Western Blotting

Western blotting was carried out using methods reported previously, with slight modification.[19] Briefly, the sample buffer (1% [w/v] sodium dodecyl sulfate [SDS], 12.5% [w/v] glycerol, 0.005% [w/v] bromophenol blue, 2.5% [w/v] 2-mercaptoethanol, and 25 mM Tris–HCl, pH 6.8) was used to dissolve 10 μg of Triton X-soluble or Triton X-insoluble samples, followed by separation on 10% to 20% (w/v) gradient

15318257, 2023, 6, Downloaded from https://movementdisorders.onlinelibrary.wiley.com/doi/10.1002/mds.29401 by Cochrane Japan, Wiley Online Library on [10/03/2024]. See the Terms and Conditions (https://onlinelibrary.wiley.com/terms-and-conditions) on Wiley Online Library for rules of use; OA articles are governed by the applicable Creative Commons License

gels (Wako, Japan). The proteins were transferred to polyvinylidene difluoride membranes (Merck Millipore, Germany), and then treated at room temperature (RT) with 4% (w/v) PFA in PBS for 30 minutes before blocking, to prevent α-syn detachment from the blotted membranes. After blocking for 1 hour with 5% [w/v] skim milk in Tris-buffered saline with 0.1% Tween 20 detergent, the membranes were incubated overnight at 4°C with primary antibodies against α-syn (1:2000; 610,787, BD Biosciences, USA), p-α-syn (1:5000; ab51253, Abcam, UK), and β-actin (1:5000; A5441, Sigma–Aldrich, USA). Subsequently, the membranes were incubated for 1 hour at RT with horseradish peroxidase-conjugated secondary antibodies (NB7574 or NB7160; Novus Biologicals, USA). A detection reagent (Thermo Fisher Scientific, USA) was used to detect immunoreactive bands, and an Amersham Imager 600 (GE Healthcare) instrument was used to detect the chemiluminescent signals. The band intensities were standardized to β-actin levels.

Primary Hippocampal Culture

Primary hippocampal E16 ICR mice cell cultures were prepared from decapitated embryos by dissecting the entire hippocampus under sterile conditions. The cells were triturated in Dulbecco's Modified Eagle's Medium (Wako, Japan) supplemented with 10% fetal bovine serum (Thermo Fisher Scientific, USA) and 1% penicillin–streptomycin (Thermo Fisher Scientific, USA) after 5 minutes of enzymatic digestion with 0.25% trypsin at 37°C. The mixture was then centrifuged at 190 × *g* for 3 minutes, and the cell pellet was immediately re-suspended in Neurobasal medium (Thermo Fisher Scientific, USA) containing 2% B27 (Invitrogen, USA), 2 mM L-glutamine (Nacalai Tesque, Japan), and 1% penicillin–streptomycin (Thermo Fisher Scientific, USA). The dissociated cells were plated on 24-well plates (1.5×10^5 cells/well) pre-coated with poly-DL-ornithine hydrobromide (Sigma–Aldrich, USA). Half of the medium was removed and replaced every 3 to 4 days. The cells were cultured in a humidified incubator at 37°C and 5% CO_2. The experiments were carried out in 14 days in vitro (DIV), and each experiment was repeated three times.

Cytotoxicity Assessment Using a Lactate Dehydrogenase Assay in the Medium

A lactate dehydrogenase (LDH) Assay Kit (Cytotoxicity LDH Assay Kit-WST, Dojindo Japan) in medium was used to assess cytotoxicity. The supernatants (100 μL) were incubated with an equal volume of assay buffer for 30 minutes, to determine the absorbance of the culture medium at a test wavelength of 490 nm using a microplate reader.

Calcium Imaging

The primary hippocampal neurons were incubated at 37°C for 1 hour in the presence of 2 μM fluo-8 AM dye (Abcam, UK). After washing twice with PBS, the medium was replaced with a fresh medium containing compounds. The cells were observed with BZ-X710 (Keyence, Japan) at 20× magnification. The fluorescence intensity was quantified using ImageJ software. The image acquisition settings were constant in all groups for each experiment.

pHrodo-PFFs, and pHrodo-Dextran Transduction

pHrodo Red (Invitrogen, USA) was used to label sonicated α-syn PFFs, as per the manufacturer's instructions. α-syn PFFs labeled with pHrodo Red (pHrodo-PFFs; final concentration: 0.5 μg/mL) and pHrodo Red-dextran (10 kDa, pHrodo-dextran; final concentration: 0.5 μg/mL; Invitrogen, USA) were added to the primary hippocampal culture at 14 DIV together with BAPTA-AM (5 μM), nitrendipine (0.025, 0.25, 2.5, or 25 μM), bepridil (0.005, 0.05, 0.5, or 5 μM), verapamil (0.02, 0.2, 2, or 20 μM), ω-agatoxin (1 μM), ω-conotoxin (5 μM), mibefradil (10 μM), SNX 482 (300 nM), W-7 (N-[6-Aminohexyl]-5-chloro-1-naphthalenesulfonamide Hydro chloride) (25 μM), trifluoperazine dihydrochloride (10 μM), CyA (0.02, 0.2, 2, or 20 μM), FK506 (0.025, 0.25, 2.5, or 25 μM), or vehicle, and incubated for 4 hours.

Statistical Analysis

The PRISM statistical package was used for statistical analysis. A Kruskal–Wallis test followed by a Dunn's post hoc test was used to assess statistical significance. The two groups of data were compared using a Mann–Whitney test, and statistical significance was set at $^*P < 0.05$, $^{**}P < 0.01$, or $^{***}P < 0.001$.

Results

Inhibition of Ca^{2+}–CaM–CaN Signaling Decreases the Neuronal Uptake of α-Syn PFFs Via Macropinocytosis

First, we assessed the involvement of intracellular Ca^{2+} in the neuronal α-syn PFFs uptake in primary hippocampal neurons. Previously, we quantified the neuronal α-syn PFFs uptake using pHrodo Red-labeled α-syn PFFs (pHrodo-PFFs).[9] Primary hippocampal neurons were transduced with pHrodo-PFFs in the presence of

15318257, 2023, 6, Downloaded from https://movementdisorders.onlinelibrary.wiley.com/doi/10.1002/mds.29401 by Cochrane Japan, Wiley Online Library on [10/03/2024]. See the Terms and Conditions (https://onlinelibrary.wiley.com/terms-and-conditions) on Wiley Online Library for rules of use; OA articles are governed by the applicable Creative Commons License

BAPTA-AM, a chelator of intracellular Ca^{2+}, or the vehicle. To rule out cytotoxicity, we measured LDH released into the conditioned medium in all of the in vitro experiments and confirmed that LDH release did not differ among them (Supplementary Figs. S1 and S2). Compared with the control group, chelation of intracellular Ca^{2+} with BAPTA-AM reduced the pHrodo-PFFs areas (Fig. 1A,B), suggesting that intracellular Ca^{2+} contributes to neuronal α-syn PFFs uptake.

Next, we investigated whether blocking VGCCs affects the neuronal uptake of α-syn PFFs. Primary hippocampal neurons were transduced with pHrodo-PFFs in the presence of L-type VGCC (nitrendipine, verapamil, and bepridil), N-type (conotoxin), P/Q-type (agatoxin), R-type (SNX 482), and T-type (mibefradil) VGCC blockers or vehicle. L-type VGCC blockers reduced the pHrodo-PFFs areas in a dose-dependent manner compared with the control, therefore, demonstrating that L-type VGCCs contribute to α-syn PFFs uptake in these neurons (Fig. 1C-E). Moreover, treatment with N-type and T-type VGCC blockers reduced the pHrodo-PFFs areas compared with the control (Fig. 2A,B). In contrast, P/Q-type and R-type VGCC blockers did not significantly reduce the pHrodo-PFFs areas (Fig. 2C,D). To elucidate the causes of the difference in the efficacy of VGCC blockers against neuronal α-syn PFFs uptake, we evaluated the efficacy of VGCC blockers against the intracellular Ca^{2+} using Ca^{2+} imaging. First, we confirmed that the administration of KCL (Potassium chloride) (50 mM) increased the fluo-8 intensity (Supplementary Fig. **S3**). Subsequently, primary hippocampal neurons were administered with KCL in the presence of VGCC blockers or the vehicle. L-type (nitrendipine, 25 μM), N-type (ω-conotoxin, 5 μM), and T-type (mibefradil, 10 μM) VGCC blockers significantly decreased the fluo-8 intensity (Supplementary Fig. **S3**). In contrast, P/Q-type (ω-agatoxin, 1 μM) and R-type (SNX 482, 300 nM) VGCC blockers did not significantly decrease the fluo-8 intensity, although there were trends toward a decrease in the intensity of fluo-8 (Supplementary Fig. **S3**), suggesting insufficient decrease in intracellular Ca^{2+}. These results suggest that the efficacy of VGCC blockers against neuronal α-syn PFFs uptake was correlated with the decrease in intracellular Ca^{2+}.

We next investigated whether blocking CaN and CaM affects the neuronal α-syn PFFs uptake. Primary hippocampal neurons were transduced with pHrodo-PFFs in the presence of CaM inhibitors (W-7 and trifluoperazine dihydrochloride), CaN inhibitors (CyA and FK506), or the vehicle. The CaM and CaN inhibitor treatments significantly decreased the pHrodo-PFFs areas compared with the control (Figs. 2E,F and 3A,B). The Ca^{2+} imaging showed that the CaM and CaN inhibitors did not affect intracellular Ca^{2+}, confirming their mechanisms of action (Supplementary Fig. S3H,I). We summarized the drugs used in Figures 1-3 and their mechanisms of action in Figure 3C. Collectively, these results suggest that Ca^{2+}–CaM–CaN signaling is strongly associated with the neuronal α-syn PFFs uptake.

Previously, we demonstrated that macropinocytosis, a type of fluid-phase endocytosis, is involved in the neuronal uptake of PFFs.[9] To investigate whether Ca^{2+}–CaM–CaN signaling is associated with macropinocytosis, we used dextran (10 kDa), which is widely used to quantify macropinocytosis.[9,20] The Ca^{2+} chelator (BAPTA-AM, 5 μM), VGCC blocker (nitrendipine, 25 μM), CaM inhibitor (W-7, 25 μM), and CaN inhibitor (CyA, 20 μM) decreased the pHrodo-dextran areas (Fig. 4A-E). These results suggest that Ca^{2+}–CaM–CaN signaling modulates macropinocytosis.

Modulation of CaN Ameliorates the Development of p-α-Syn-Positive Pathology in a Mouse PD Model

We explored whether modulating Ca^{2+}–CaM–CaN signaling using a CaN inhibitor, CyA, affects the propagation of α-syn pathology in a mouse PD model. First, we validated the efficacy of oral administration of the CaN inhibitor by evaluating the CaN level in the brains of mice treated with CyA. Previous studies showed that the oral administration of CyA decreased CaN activity in mouse brains and modulated the brain pathology in an Alzheimer's disease model.[21,22] Wild-type (WT) mice were treated orally with CyA or vehicle for 1 week, and the CaN activity in the mouse brains was examined. CyA administration reduced CaN activity in a time-dependent manner compared with control (Fig. 5A,B). Next, we analyzed the expression levels of α-syn and p-α-syn in mouse brains to exclude the possibility that the CyA administration could affect these proteins. Western blot analysis revealed that CyA did not significantly affect the expression levels of total α-syn and p-α-syn (Fig. 5C,D).

We also examined whether modulating CaN ameliorates the α-syn pathology in an in vivo PD model previously established by our group.[9,15] We analyzed the effect of the oral administration of CyA or vehicle to WT mice inoculated with α-syn PFFs into the OB bilaterally by stereotaxic injection. CyA treatment began before α-syn PFFs injection, and mice were sacrificed 2 weeks after the injection (Fig. 5E). We analyzed the areas of p-α-syn-positive pathology and the number of neuronal p-α-syn-positive aggregates in the AON, as described previously.[9,15] The areas of p-α-syn-positive pathology and number of neuronal p-α-syn-positive aggregates in the AON were significantly decreased in

15318257, 2023, 6, Downloaded from https://movementdisorders.onlinelibrary.wiley.com/doi/10.1002/mds.29401 by Cochrane Japan, Wiley Online Library on [10/03/2024]. See the Terms and Conditions (https://onlinelibrary.wiley.com/terms-and-conditions) on Wiley Online Library for rules of use; OA articles are governed by the applicable Creative Commons License

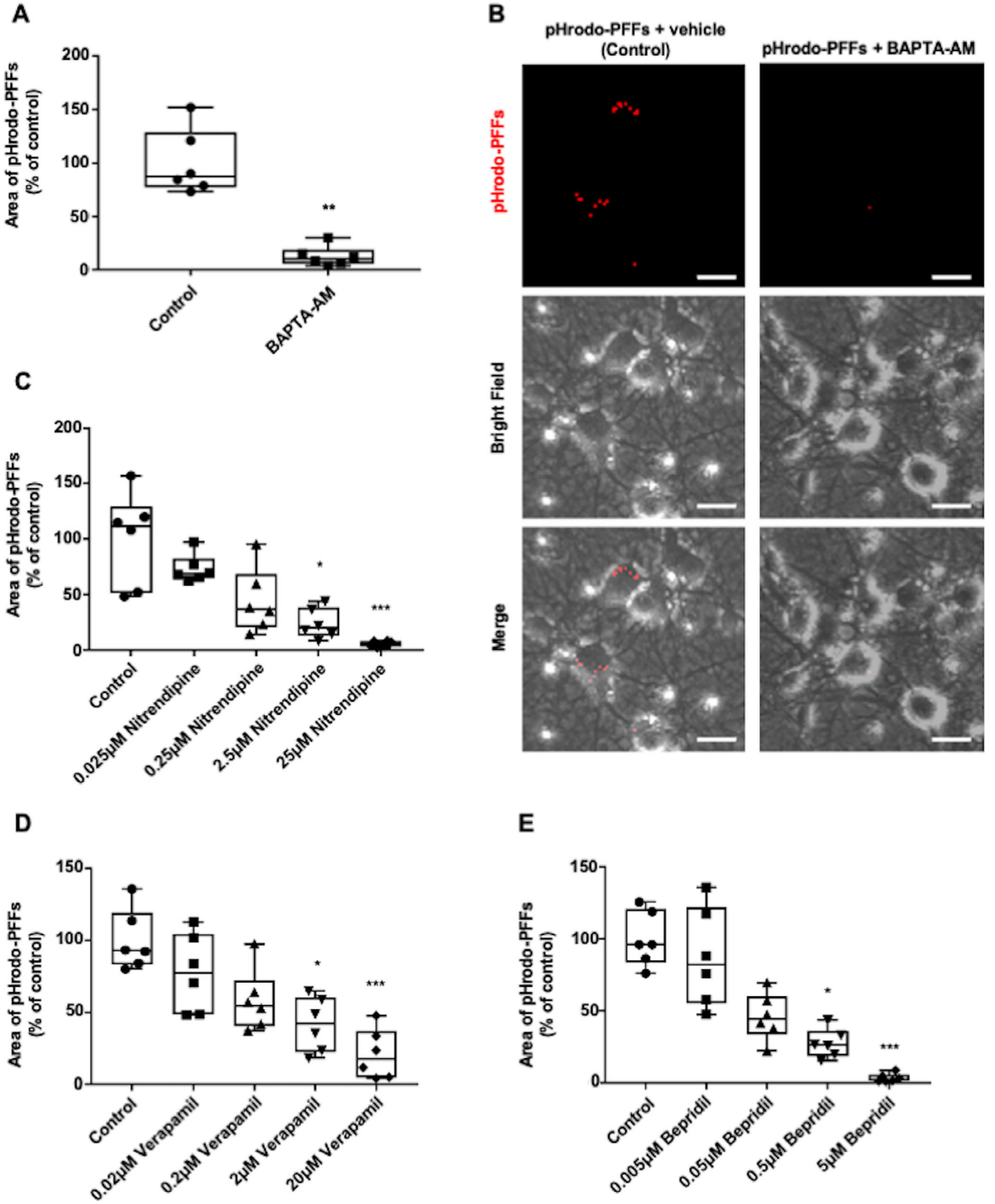

FIG. 1. Ca^{2+} chelator and L-type voltage-gated Ca^{2+} channels blockers inhibit the α-synuclein preformed fibrils (PFFs) uptake in primary hippocampal neurons. (A,C-E) pHrodo-PFFs areas in primary hippocampal neurons. Data were representative of three independent experiments (n = 6). Data were reported as box plots and were normalized against the control. $^{**}P < 0.01$, $^{***}P < 0.001$, Mann–Whitney test (A) or Kruskal–Wallis test and Dunn's post hoc test (C-E). Scatter plots showed data from each sample. (B) Representative images of pHrodo-PFFs in primary hippocampal neurons. Data were representative of three independent experiments. Scale bar: 20 μm. [Color figure can be viewed at wileyonlinelibrary.com]

15318257, 2023, 6, Downloaded from https://movementdisorders.onlinelibrary.wiley.com/doi/10.1002/mds.29401 by Cochrane Japan, Wiley Online Library on [10/03/2024]. See the Terms and Conditions (https://onlinelibrary.wiley.com/terms-and-conditions) on Wiley Online Library for rules of use; OA articles are governed by the applicable Creative Commons License

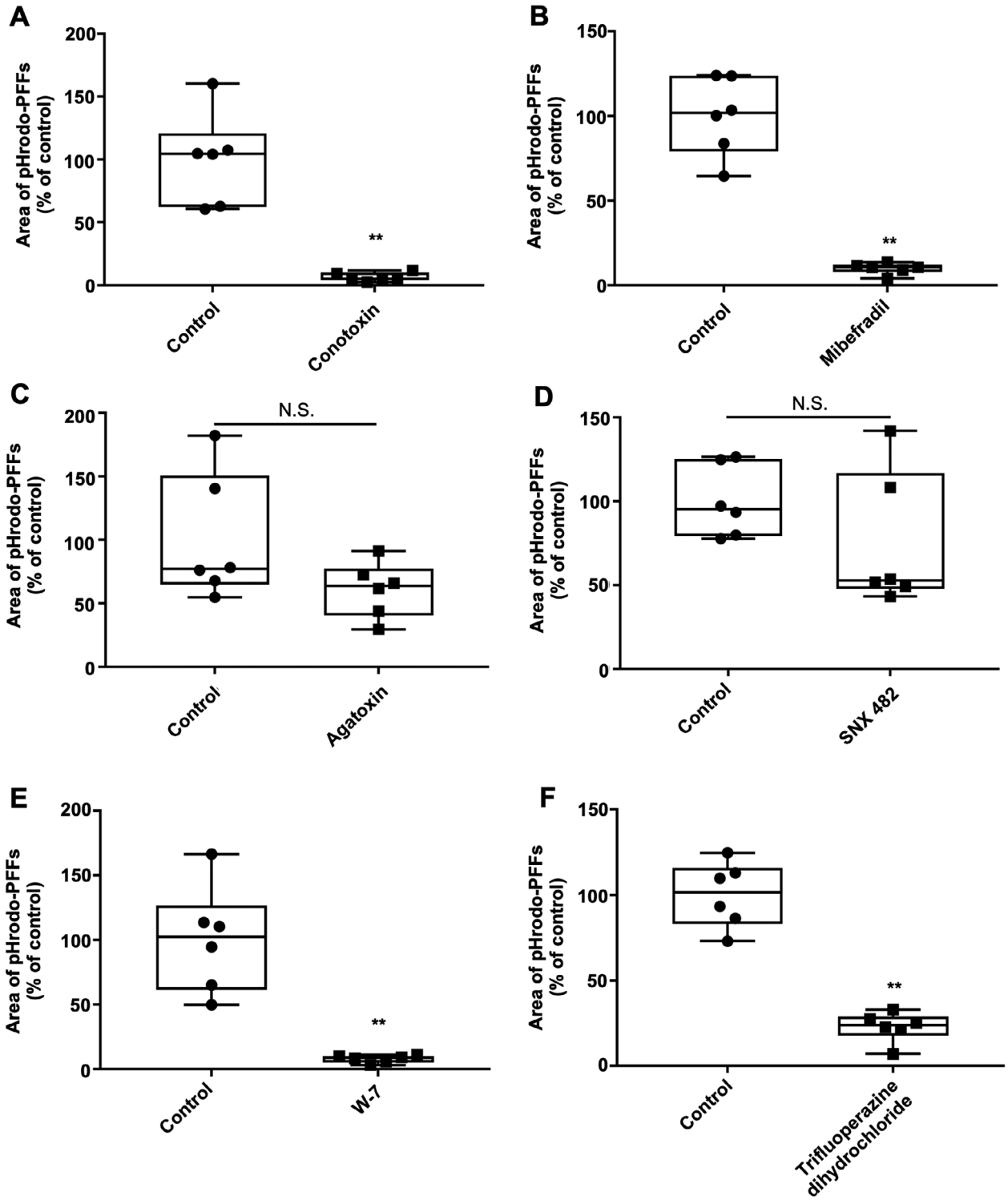

FIG. 2. N-type voltage-gated Ca2+ channels (VGCC) blockers, T-type VGCC blockers, and calmodulin (CaM) inhibitors inhibit the α-synuclein preformed fibrils (PFFs) uptake in primary hippocampal neurons. (A-F) pHrodo-PFFs areas in primary hippocampal neurons. Data were obtained from three independent experiments (n = 6). Data were reported as box plots and were normalized against the control. ***$P < 0.001$, N.S.: not significant, Mann–Whitney test. Scatter plots showed data from each sample.

mice treated with CyA compared with those in control mice (Fig. 5F-H). Subsequently, using a Western blot analysis, we quantified the amount of p-α-syn-positive aggregates. In accordance with the immunohistochemical results, Western blot analysis showed significantly decreased p-α-syn in the Triton X-insoluble fraction of

15318257, 2023, 6, Downloaded from https://movementdisorders.onlinelibrary.wiley.com/doi/10.1002/mds.29401 by Cochrane Japan, Wiley Online Library on [10/03/2024]. See the Terms and Conditions (https://onlinelibrary.wiley.com/terms-and-conditions) on Wiley Online Library for rules of use; OA articles are governed by the applicable Creative Commons License

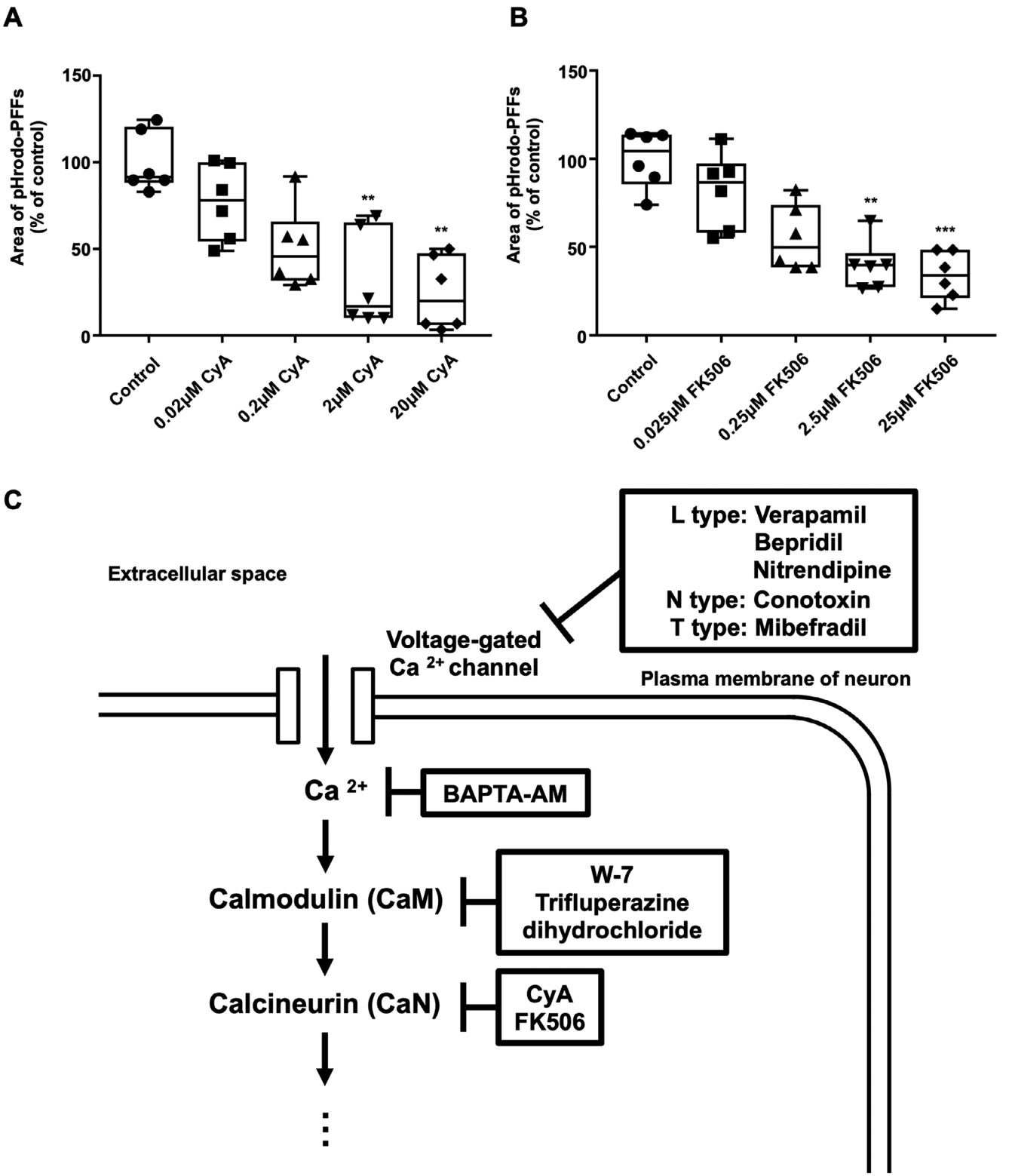

FIG. 3. Calcineurin (CaN) inhibitors inhibit the α-synuclein preformed fibrils (PFFs) uptake in primary hippocampal neurons. (A,B) pHrodo-PFFs areas in primary hippocampal neurons. Data were representative of three independent experiments (n = 6). Data were reported as box plots and were normalized against the control. $^{**}P < 0.01$, $^{***}P < 0.001$, N.S.: not significant, Kruskal–Wallis test and Dunn's post hoc test. Scatter plots showed data from each sample. (C) Summary of the drugs used in Figures 1-3 and their mechanisms of action.

mice treated with CyA compared with the control (Fig. 5I). We also examined the effects of CyA administration on astrocytic and microglial activation, which may affect the development of neuronal α-syn pathology.[23,24] Immunohistochemical analyses showed that the expression levels of GFAP and Iba-1 significantly

15318257, 2023, 6, Downloaded from https://movementdisorders.onlinelibrary.wiley.com/doi/10.1002/mds.29401 by Cochrane Japan, Wiley Online Library on [10/03/2024]. See the Terms and Conditions (https://onlinelibrary.wiley.com/terms-and-conditions) on Wiley Online Library for rules of use; OA articles are governed by the applicable Creative Commons License

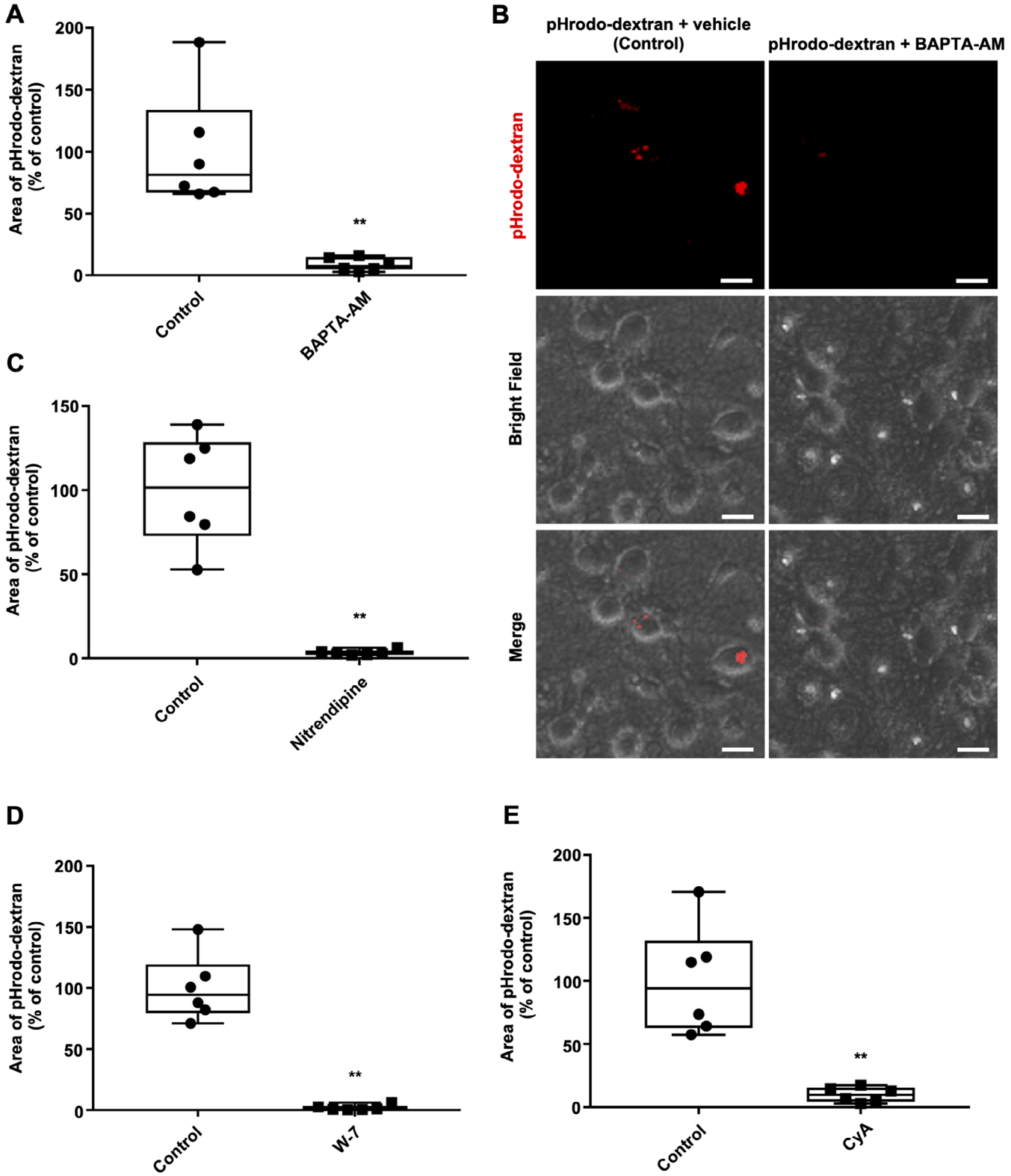

FIG. 4. Ca^{2+} chelator, L-type voltage-gated Ca2+ channels blocker, calmodulin (CaM) inhibitor, and calcineurin (CaN) inhibitor inhibit macropinocytosis. (A,C-E) pHrodo-dextran areas in primary hippocampal neurons. Data were representative of three independent experiments (n = 6). Data were reported as box plots and were normalized against the control. ***$P < 0.001$, Mann–Whitney test. Scatter plots showed data from each sample. (B) Representative images of pHrodo-dextran in primary hippocampal neurons. Data were representative of three independent experiments. Scale bar: 20 μm. [Color figure can be viewed at wileyonlinelibrary.com]

15318257, 2023, 6, Downloaded from https://movementdisorders.onlinelibrary.wiley.com/doi/10.1002/mds.29401 by Cochrane Japan, Wiley Online Library on [10/03/2024]. See the Terms and Conditions (https://onlinelibrary.wiley.com/terms-and-conditions) on Wiley Online Library for rules of use; OA articles are governed by the applicable Creative Commons License

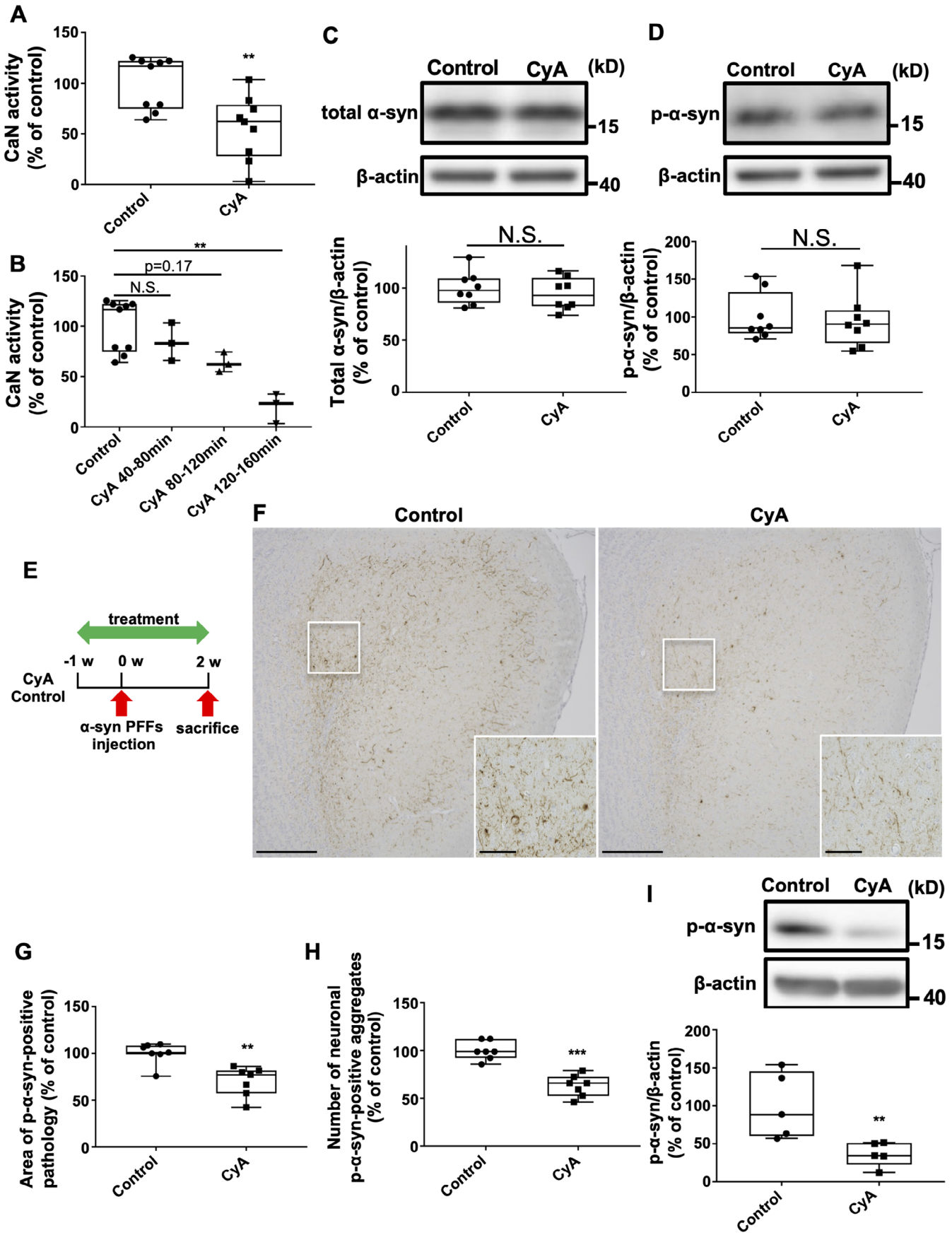

FIG. 5. Legend on next page.

15318257, 2023, 6, Downloaded from https://movementdisorders.onlinelibrary.wiley.com/doi/10.1002/mds.29401 by Cochrane Japan, Wiley Online Library on [10/03/2024]. See the Terms and Conditions (https://onlinelibrary.wiley.com/terms-and-conditions) on Wiley Online Library for rules of use; OA articles are governed by the applicable Creative Commons License

increased in mice injected with α-syn PFFs as compared with mice injected with PBS (Fig. S4). However, CyA administration did not significantly affect the expression levels of GFAP and Iba-1 in mice injected with α-syn PFFs (Supplementary Fig. S4).

Discussion

Although several studies have reported the reduction of neuronal α-syn PFFs uptake by inhibition of neuronal activity, the underlying mechanisms remain unclear. Here, we used in vitro and in vivo PD models to demonstrate that Ca^{2+}–CaM–CaN signaling plays a crucial role in the neuronal α-syn PFFs uptake. We found that the modulation of Ca^{2+}–CaM–CaN signaling inhibited the neuronal α-syn PFFs uptake via macropinocytosis. Previous studies demonstrated that PFFs taken up by neurons are transported to lysosomes and multivesicular bodies, contributing to endogenous α-syn aggregation and exosomal transmission to naive cells.[25,26] Moreover, similar to our in vitro results, our in vivo results suggest that CaN modulation inhibits the development of p-α-syn pathology induced by α-syn PFFs.

This study yielded several important findings. First, our results strongly suggest that Ca^{2+}–CaM–CaN signaling affects the neuronal α-syn PFFs uptake. The correlation between endocytosis and Ca^{2+}–CaM–CaN signaling, especially CaN, has been previously reported.[12,13] CaN was initially isolated from nervous tissues as an enzyme that is activated by Ca^{2+}/CaM. Moreover, CaN is a downstream target of the Ca^{2+}/CaM complex, activated by VGCC-mediated Ca^{2+} influx. In turn, activated CaN dephosphorylates a set of nerve-terminal proteins called dephosphins, such as dynamin 1 and synaptojanin, which are essential for endocytosis.[12,13] Considering that CaN activity is typically engaged in the somatodendritic region of neurons,[27] inhibition of neuronal α-syn PFFs uptake via CaN inhibitors may occur mainly in neuronal soma and dendrites rather than in axons. Previously, clinical studies demonstrated that immunosuppression therapy reduced the risk of PD.[28,29] However, because the immunosuppressants used in these studies included not only CaN inhibitors, but also other immunosuppressants, such as azathioprine and methotrexate, the correlation between CaN inhibitors alone and the risk of PD remains unknown. Although our results indicate that Ca^{2+}–CaM–CaN signaling could be a promising therapeutic target, additional research is needed to determine the most promising target in Ca^{2+}–CaM–CaN signaling pathway, as well as the effects of Ca^{2+}–CaM–CaN signaling inhibitors on other features of PD models, such as neuronal death and behavioral changes.

Second, we showed that Ca^{2+}–CaM–CaN signaling modulates macropinocytosis. Macropinocytosis is a type of fluid-phase endocytosis that is characterized by the formation of large endocytic vesicles. Previous studies have suggested that macropinocytosis is affected by intracellular Ca^{2+} and CaN activity,[30,31] which supports our results.

Third, we demonstrated that the inhibition of L-type, N-type, and T-type VGCCs reduced the neuronal uptake of α-syn PFFs, whereas the inhibition of P/Q-type and R-type VGCCs did not, which could be correlated with decrease in intracellular Ca^{2+}. VGCCs are classified into five subtypes (L-, N-, P/Q-, R-, and T-type channels), whose functions and distribution differ within neurons.[32,33] Interestingly, a previous study showed that neuronal activity-dependent Ca^{2+} influx was inhibited to a greater extent by an N-type VGCC blocker than by a P/Q-type VGCC blocker,[34] which is consistent with our results.

Recently, we showed that PER treatment inhibits neuronal α-syn PFFs uptake.[12] AMPA treatment elevates intracellular Ca^{2+} by increasing Ca^{2+} influx through VGCCs and Ca^{2+}-permeable AMPA receptors,[35,36] whereas PER treatment inhibits AMPA-induced Ca^{2+} influx in primary neurons.[37] Therefore, the efficacy of PER against the neuronal uptake of α-syn PFFs may be attributed to the inhibition of Ca^{2+} influx in neurons. Notably, previous studies reported the beneficial effect of a VGCC blocker, isradipine, in experimental PD models.[38,39] Although a clinical trial of isradipine in patients with PD narrowly failed to

FIG. 5. Inhibition of calcineurin (CaN) reduces the development of phosphorylated α- synuclein (p-α-syn)-positive pathology in a mouse Parkinson's disease model. (A) CaN activity in the brains of mice treated with cyclosporin A (CyA) (n = 9). All values were expressed as box plots. $^{**}P < 0.01$, Mann–Whitney test. Plotted data were normalized against control. (B) Change in CaN activity at 40 to 80 minutes (n = 3), 80 to 120 minutes (n = 3), or 120to 160 minutes (n = 3) after the oral administration of CyA. Plotted data were normalized against control. All values were expressed as box plots. $^{***}P < 0.001$, N.S.: not significant, Kruskal–Wallis test and Dunn's post hoc test. (C,D) Total α-syn (C) and p-α-syn (D) levels in the Triton X-soluble fraction. The positions of size markers were indicated by the numbers (in kDa) to the right of the image. Representative images and plotted data were shown (n = 8). All values were expressed as box plots. N.S.: not significant, Mann–Whitney test. (E) Time schedule for the injection of α-syn preformed fibrils (PFFs) and drug treatment. (F) Representative images of the immunohistochemical staining of the mice that underwent α-syn PFFs injection and CyA treatment. The insets showed high-power images of the p-α-syn-positive pathology in the anterior olfactory nucleus (AON). Scale bar: 200 μm; inset: 50 μm. (G) Area of p-α-syn-positive pathology in the AON (n = 7). Data were expressed as box plots and were normalized against the control. $^{**}P < 0.01$, Mann–Whitney test. (H) Number of neuronal p-α-syn-positive aggregates in the AON (n = 7). Data were expressed as box plots and were normalized against the control. $^{***}P < 0.001$, Mann–Whitney test. (I) Level of p-α-syn in the Triton X-insoluble fraction. The positions of size markers were indicated by the numbers (in kDa) to the right of the image. Representative images and plotted data were shown (n = 5). All values were expressed as box plots. $^{*}P < 0.05$, Mann–Whitney test. [Color figure can be viewed at wileyonlinelibrary.com]

15318257, 2023, 6, Downloaded from https://movementdisorders.onlinelibrary.wiley.com/doi/10.1002/mds.29401 by Cochrane Japan, Wiley Online Library on [10/03/2024]. See the Terms and Conditions (https://onlinelibrary.wiley.com/terms-and-conditions) on Wiley Online Library for rules of use; OA articles are governed by the applicable Creative Commons License

meet its primary endpoint,[40,41] our results support the potential of isradipine as a disease-modifying drug of PD.

This study has several limitations. First, in the in vivo study, we evaluated the efficacy of CyA against α-syn pathology formation in the AON, the first-order brain region from the injection site, at 2 weeks post-injection. In a future study, we will evaluate α-syn pathology in the second- or higher-order brain regions with prolonged incubation to examine the efficacy of modulating Ca^{2+}–CaM–CaN signaling against neuron-to-neuron transmission of pathological α-syn. Second, the VGCC inhibitors block glutamate release and hence, suppress neuronal activity.[42,43] Therefore, it is possible that the inhibition of neuronal α-syn PFFs uptake was caused not only by inhibiting Ca^{2+} influx, but also by suppressing neuronal activity. Third, although neuronal activity was reported to affect the affinity of dihydropyridines for L-type VGCC,[44] we did not evaluate this point in this study. Therefore, it would be intriguing to elucidate the correlation between neuronal activity, the effect of dihydropyridines on PFFs uptake, and α-syn pathology formation in further studies.

In conclusion, this study demonstrated that the modulation of Ca^{2+}–CaM–CaN signaling inhibited the neuronal α-syn PFFs uptake via macropinocytosis and the subsequent development of p-α-syn-positive pathology in PD models. Our results support the hypothesis that Ca^{2+}–CaM–CaN signaling modulates α-syn transmission and that targeting Ca^{2+}–CaM–CaN signaling is a promising therapeutic strategy for PD. ●

Acknowledgments: We thank Ms. Rie Hikawa for the technical assistance.

Data Availability Statement

The data that support the findings of this study are available from the corresponding author upon reasonable request.

References

1. Braak H, Del Tredici K, Rüb U, de Vos RA, Jansen Steur EN, Braak E. Staging of brain pathology related to sporadic Parkinson's disease. Neurobiol Aging 2003;24:197–211.
2. Olanow CW, Prusiner SB. Is Parkinson's disease a prion disorder? Proc Natl Acad Sci 2009;106:12571–12572.
3. Lee SJ, Desplats P, Lee HJ, Spencer B, Masliah E. Cell-to-cell transmission of α-synuclein aggregates. Methods Mol Biol 2012;849:347–359.
4. Luk KC, Kehm V, Carroll J, et al. Pathological α-synuclein transmission initiates Parkinson-like neurodegeneration in nontransgenic mice. Science 2012;338:949–953.
5. Masuda-Suzukake M, Nonaka T, Hosokawa M, et al. Prion-like spreading of pathological α-synuclein in brain. Brain 2013;136:1128–1138.
6. Guo JL, Lee VM. Cell-to-cell transmission of pathogenic proteins in neurodegenerative diseases. Nat Med 2014;20:130–138.
7. Dehay B, Vila M, Bezard E, Brundin P, Kordower JH. Alpha-synuclein propagation: new insights from animal models. Mov Disord 2016;31:161–168.
8. Volpicelli-Daley LA, Luk KC, Patel TP, et al. Exogenous α-synuclein fibrils induce Lewy body pathology leading to synaptic dysfunction and neuron death. Neuron 2011;72:57–71.
9. Ueda J, Uemura N, Sawamura M, et al. Perampanel inhibits α-synuclein transmission in parkinson's disease models. Mov Disord 2021;36:1554–1564.
10. Wu Q, Shaikh MA, Meymand ES, et al. Neuronal activity modulates alpha-synuclein aggregation and spreading in organotypic brain slice cultures and in vivo. Acta Neuropathol 2020;140:831–849.
11. Imamura Y, Okuzumi A, Yoshinaga S, et al. Quantum-dot-labeled synuclein seed assay identifies drugs modulating the experimental prion-like transmission. Commun Biol 2022;29:636.
12. Wu XS, Zhang Z, Zhao WD, et al. Calcineurin is universally involved in vesicle endocytosis at neuronal and nonneuronal secretory cells. Cell Rep 2014;22:982–988.
13. Cousin MA. Synaptic vesicle endocytosis: calcium works overtime in the nerve terminal. Mol Neurobiol 2000;22:115–128.
14. Uemura N, Yagi H, Uemura MT, Hatanaka Y, Yamakado H, Takahashi R. Inoculation of α-synuclein preformed fibrils into the mouse gastrointestinal tract induces Lewy body-like aggregates in the brainstem via the vagus nerve. Mol Neurodegener 2018;13:21.
15. Uemura N, Uemura MT, Lo A, et al. Slow progressive accumulation of oligodendroglial alpha-synuclein (α-syn) pathology in synthetic α-syn fibril-induced mouse models of synucleinopathy. J Neuropathol Exp Neurol 2019;78:877–890.
16. Uemura N, Ueda J, Yoshihara T, et al. α-Synuclein spread from olfactory bulb causes hyposmia, anxiety, and memory loss in BAC-SNCA mice. Mov Disord 2021;36:2036–2047.
17. Li SY, Nelson DS. Effects of cyclosporin a on the production of experimental anti-erythrocyte autoantibodies in mice. Int J Immunopharmacol 1986;8:213–219.
18. Taguchi T, Ikuno M, Hondo M, et al. α-Synuclein BAC transgenic mice exhibit RBD-like behaviour and hyposmia: a prodromal Parkinson's disease model. Brain 2020;143:249–265.
19. Uemura N, Koike M, Ansai S, et al. Viable neuronopathic Gaucher disease model in Medaka (Oryzias latipes) displays axonal accumulation of alpha-synuclein. PLoS Genet 2015;11:e1005065.
20. Rey NL, Steiner JA, Maroof N, et al. Widespread transneuronal propagation of α-synucleinopathy triggered in olfactory bulb mimics prodromal Parkinson's disease. J Exp Med 2016;213:1759–1778.
21. Liu H, Tu L, Wang Q, et al. Modulation of calcineurin activity in mouse brain by chronic oral administration of cyclosporine A. IUBMB Life 2013;65:445–453.
22. Ding Y, Zhong Y, Baldeshwiler A, et al. Protecting P-glycoprotein at the blood-brain barrier from degradation in an Alzheimer's disease mouse model. Fluids Barriers CNS 2021;18:10.
23. Tsunemi T, Ishiguro Y, Yoroisaka A, et al. Astrocytes protect human dopaminergic neurons from α-synuclein accumulation and propagation. J Neurosci 2020;40:8618–8628.
24. Bido S, Muggeo S, Massimino L, et al. Microglia-specific overexpression of α-synuclein leads to severe dopaminergic neurodegeneration by phagocytic exhaustion and oxidative toxicity. Nat Commun 2021;12:6237.
25. Flavin WP, Bousset L, Green ZC, et al. Endocytic vesicle rupture is a conserved mechanism of cellular invasion by amyloid proteins. Acta Neuropathol 2017;134:629–653.
26. Bayati A, Banks E, Han C, et al. Rapid macropinocytic transfer of α-synuclein to lysosomes. Cell Rep 2022;40:111102.
27. Fujii H, Inoue M, Okuno H, et al. Nonlinear decoding and asymmetric representation of neuronal input information by CaMKIIα and calcineurin. Cell Rep 2013;3:978–987.
28. Camacho-Soto A, Gross A, Nielsen SS, Dey N, Racette BA. Inflammatory bowel disease and risk of Parkinson's disease in Medicare beneficiaries. Parkinsonism Relat Disord 2018;50:23–28.

15318257, 2023, 6, Downloaded from https://movementdisorders.onlinelibrary.wiley.com/doi/10.1002/mds.29401 by Cochrane Japan, Wiley Online Library on [10/03/2024]. See the Terms and Conditions (https://onlinelibrary.wiley.com/terms-and-conditions) on Wiley Online Library for rules of use; OA articles are governed by the applicable Creative Commons License

29. Guo X, Chong L, Zhang X, Li R. Immunosuppressants contribute to a reduced risk of Parkinson's disease in rheumatoid arthritis. Int J Epidemiol 2022;51:1328–1338.

30. Janzen E, Mendoza-Ferreira N, Hosseinibarkooie S, et al. CHP1 reduction ameliorates spinal muscular atrophy pathology by restoring calcineurin activity and endocytosis. Brain 2018;141:2343–2361.

31. Kabayama H, Nakamura T, Takeuchi M, et al. Ca^{2+} Induces macropinocytosis via F-Actin depolymerization during growth cone collapse. Mol Cell Neurosci 2009;40:27–38.

32. Pardo NE, Hajela RK, Atchison WD. Acetylcholine release at neuromuscular junctions of adult tottering mice is controlled by N-(cav2.2) and R-type (cav2.3) but not L-type (cav1.2) Ca^{2+} channels. J Pharmacol Exp Ther 2006;319:1009–1020.

33. Scamps F, Vigues S, Restituito S, et al. Sarco-endoplasmic ATPase blocker 2,5-Di(tert-butyl)-1, 4-benzohydroquinone inhibits N-, P-, and Q- but not T-, L-, or R-type calcium currents in central and peripheral neurons. Mol Pharmacol 2000;58:18–26.

34. Kim SH, Ryan TA. Balance of calcineurin Aα and CDK5 activities sets release probability at nerve terminals. J Neurosci 2013;33:8937–8950.

35. Thiagarajan TC, Lindskog M, Tsien RW. Adaptation to synaptic inactivity in hippocampal neurons. Neuron 2005;47:725–737.

36. Plant K, Pelkey KA, Bortolotto ZA, et al. Transient incorporation of native GluR2-lacking AMPA receptors during hippocampal long-term potentiation. Nat Neurosci 2006;9:602–604.

37. Hanada T, Hashizume Y, Tokuhara N, et al. Perampanel: a novel, orally active, noncompetitive AMPA-receptor antagonist that reduces seizure activity in rodent models of epilepsy. Epilepsia 2011;52:1331–1340.

38. Chan CS, Guzman JN, Ilijic E, et al. 'Rejuvenation' protects neurons in mouse models of Parkinson's disease. Nature 2007;447:1081–1086.

39. Ilijic E, Guzman JN, Surmeier DJ. The L-type channel antagonist isradipine is neuroprotective in a mouse model of Parkinson's disease. Neurobiol Dis 2011;43:364–371.

40. Parkinson Study Group STEADY-PD III Investigators. Isradipine versus placebo in early Parkinson disease: a randomized trial. Ann Intern Med 2020;172:591–598.

41. Surmeier DJ, Nguyen JT, Lancki N, et al. Re-analysis of the STEADY-PD II trial-evidence for slowing the progression of Parkinson's disease. Mov Disord 2022;37:334–342.

42. Schmitz Y, Witkovsky P. Dependence of photoreceptor glutamate release on a dihydropyridine-sensitive calcium channel. Neuroscience 1997;78:1209–1216.

43. Turner TJ, Dunlap K. Pharmacological characterization of presynaptic calcium channels using subsecond biochemical measurements of synaptosomal neurosecretion. Neuropharmacology 1995;34:1469–1478.

44. Wei XY, Rutledge A, Triggle DJ. Voltage-dependent binding of 1,4-dihydropyridine Ca^{2+} channel antagonists and activators in cultured neonatal rat ventricular myocytes. Mol Pharmacol 1989;35:541–552.

Supporting Data

Additional Supporting Information may be found in the online version of this article at the publisher's web-site.

15318257, 2023, 6, Downloaded from https://movementdisorders.onlinelibrary.wiley.com/doi/10.1002/mds.29401 by Cochrane Japan, Wiley Online Library on [10/03/2024]. See the Terms and Conditions (https://onlinelibrary.wiley.com/terms-and-conditions) on Wiley Online Library for rules of use; OA articles are governed by the applicable Creative Commons License